

# Control of the structure and properties of barium sulphate-filled blends of polypropylene and ethylene propylene copolymers

C. O. HAMMER, F. H. J. MAURER\*

*Chalmers University of Technology, Department of Polymer Technology,  
S-41296 Gothenburg, Sweden  
E-mail: frans.maurer@polymer.lth.se*

S. MOLNÁR, B. PUKÁNSZKY

*Technical University of Budapest, Department of Plastics and Rubber Technology,  
H-1521 Budapest, P.O. Box 92, Hungary  
E-mail: pukanszky.mua@chem.bme.hu*

The structure and properties of polypropylene (PP) and ethylene propylene copolymer (EPR) blends filled with BaSO<sub>4</sub> have been investigated. The aspect of structure control concerned was the separate dispersion of filler and rubber in the PP matrix or encapsulation of the filler in the rubber phase. The former structure prevails in the PP/EPR/BaSO<sub>4</sub> systems, and addition of maleic anhydride-grafted polypropylene (MAPP) enhances the adhesion between the PP matrix and the filler. Encapsulation of the filler particles into the elastomer takes place when maleated EPR-rubber (EPMA) is used, and the encapsulated structure prevails even under the severe shearing conditions of injection molding. The improved matrix/filler adhesion resulted in increased yield stress and tensile strength, but decreased impact resistance. The particle size of the filler proved to be a crucial factor; below a certain particle size aggregation becomes a dominating factor. Extensive aggregation leads to the deterioration of all mechanical properties, especially to decreased impact strength. © 1999 Kluwer Academic Publishers

## 1. Introduction

In the last few years the production and use of polypropylene has shown the highest growth rate among all commodity polymers. By the year 2000 the volume of production is expected to exceed that of the total amount of polyethylene. The success of this polymer is due to its extremely advantageous price/performance/volume ratio and to its versatility. With the appropriate modification, the properties of this polymer can cover a very wide range from soft elastomeric materials to engineering thermoplastics [1].

A considerable amount of PP is used as bumper compound in the automotive industry [2–4]. These compounds must meet very stringent requirements, the most important of which are the high impact strength and sufficient stiffness. The impact resistance of PP can be increased by the introduction of elastomers, but this modification leads to a decrease in modulus. On the other hand, fillers increase stiffness, but usually decrease impact resistance. As a consequence, bumper compounds frequently contain both components.

Due to their great practical importance, three-component PP/elastomer/filler compounds have received

much attention in recent years [5–10]. Considerable efforts have been concentrated on the determination of the structure/property correlations of these materials. It has been shown that two characteristic morphologies can develop in these three-component systems: independent, separate dispersion of the components, on the one hand, and encapsulation of the filler into the elastomer, on the other [11]. Attempts have been made to produce composites with exclusive structures, but these failed in most cases. In spite of the efforts made, no clear picture was obtained of the structure/property correlations of these systems, and the most diverse, usually contradictory, opinions are published in the literature.

The goal of our research was to obtain additional information about the factors influencing the structure and properties of PP/elastomer/filler composites. The principles of structure control used in this study were experimentally determined in earlier work [12–14], in which the interaction of the components was controlled by the use of functionalized polymers. The effect of filler particle size has also been studied. Since the experiments in this study were carried out on injection

\* To whom correspondence should be addressed.

Present address: Lund University, Institute of Technology, Department of Polymer Science & Engineering, Center for Chemistry and Chemical Engineering, SE-22100 Lund, Sweden.

molded samples, the results have direct practical relevance.

## 2. Preliminary considerations

PP composites are invariably prepared by the homogenization of the components in the molten state. The structure of the composites is determined by the relative magnitude of forces promoting the encapsulation of the filler particles or the separate dispersion of the components, respectively. It has been shown previously that thermodynamics favors encapsulation [11, 15]. The interaction of the components is determined by the particle size of the filler and surface energetics [16, 17], i.e.

$$F_a = \frac{3}{2}\pi W_{AB}R_a \quad (1)$$

where  $F_a$  is the adhesive force between two particles,  $W_{AB}$  is the reversible work of adhesion and  $R_a = R_1 R_2 / (R_1 + R_2)$ , an effective radius, when the size of the two interacting particles is different. Although Equation 1 was developed to describe the interaction of two particles, it can be successfully adapted for the present case: the encapsulation of a filler particle by the elastomer [11]. During homogenization hydrodynamic forces separate the components, which can be described by [17, 18]

$$F_h = -6.12\pi\eta R^2\dot{\gamma} \quad (2)$$

where  $\eta$  is the viscosity of the melt and  $\dot{\gamma}$  is the shear rate. Similarly to Equation 1, this equation can also be applied in the present case. The prevailing morphology is determined by the relative magnitude of the two forces:

$$\frac{F_a}{F_h} = k \frac{W_{AB}}{\eta\dot{\gamma}_0 R} \quad (3)$$

It is clear that strong adhesion leads to encapsulation, and decreased particle size and low shear rate have basically the same effect. As a consequence, the three important factors determining structure are adhesion, particle size and shear stress. The effect of the first two factors is the subject of this paper: adhesion is changed by the application of functionalized polymers, and three fillers with different average particle sizes were used in the experiments.

However, industrial fillers usually have a relatively wide particle size distribution. As a result, exclusive structures, i.e. complete encapsulation or separate dispersion, cannot usually be achieved, large particles are

usually dispersed separately, while the probability of encapsulation is larger for small particles. In spite of its importance, the extent of encapsulation is determined in very limited cases [15, 19]. Only a few papers discuss this question, and the existence of exclusive structures is not proved even when their formation is claimed. The extent of encapsulation can be estimated from the changes of modulus with composition by using theoretical models; it can be calculated from self-consistent models including the existence of an interlayer [20], or even from the simple Lewis-Nielsen model [15, 19]. A similar approach can be followed by using tensile yield stress values [19], although the estimate is less accurate and more assumptions must be made in order to arrive to an acceptable conclusion. However, in this paper we will only consider the experimental results and qualitatively investigate the structure in the complicated PP/EPR/BaSO<sub>4</sub> systems studied here.

## 3. Experimental

The Stamylan P16M10 grade PP homopolymer of DSM, The Netherlands, was chosen as matrix polymer, while Exxelor PE 808 of Exxon was used as the elastomer component. Preferential adhesion was achieved by the use of functionalized components. A maleinated PP (Hostaprime HC5, Hoechst) was applied to improve adhesion of filler to the PP phase, while a maleinated elastomer (Exxelor VA1810) was selected to promote encapsulation into the elastomer phase. The most important properties of the polymers are listed in Table I. Molecular weights were determined by Size Exclusion Chromatography (SEC) in tetrachlorobenzene (TCB) at 135 °C by using PE standards. The heat of fusion,  $\Delta H$  [J/g], of the two PP polymers was measured by differential scanning calorimetry (DSC) on a Perkin-Elmer 7 DSC, with a heating rate of 10 °C/min. The second heating run was used. Three precipitated BaSO<sub>4</sub> fillers, all produced by Sachtleben, Germany, were selected for the study. They differed in average particle size; the Blanc Fixe F grade had a particle size of 1.0  $\mu\text{m}$ , the Blanc Fixe Micro grade was somewhat smaller (0.7  $\mu\text{m}$ ), while the particles of the Sachtoperse HU had the smallest dimensions (0.1  $\mu\text{m}$ ).

Altogether 17 composites and reference systems were investigated; their composition is compiled in Table II. The composites were homogenized on a Werner-Pfleiderer corotating twin screw extruder with an L/D ratio of 32 and screw diameter of 30 mm at 220 °C. Mechanical testing and dynamic mechanical

TABLE I The most important characteristics of the polymers used in the study

Polymer	Producer	Code	MFI <sup>a</sup> (g/10 min)	$M_n$ (kg/mol)	$M_w$ (kg/mol)	Heat of fusion (J/g)	Density <sup>a</sup> (g/cm <sup>3</sup> )
Stamylan P16M10	DSM	PP	5.5 <sup>b</sup>	31	216	98	0.91
Hostaprime HC5	Hoechst	MAPP	—	8.4	25	69	0.9
Exxelor PE 808	Exxon	EPR	5 <sup>c</sup>	34.7	173	—	0.87
Exxelor VA 1810	Exxon	EPMA	7.5 <sup>c</sup>	28.5	120	—	0.87

<sup>a</sup>According to the manufacturer. <sup>b</sup>(230 °C, 21.2 N). <sup>c</sup>(230 °C, 10 kg).

TABLE II Composition of the investigated composites and reference compounds

Components	Composition (vol %)	MAPP <sup>a</sup> (%)	Particle size ( $\mu\text{m}$ )
PP/EPR/BaSO <sub>4</sub>	70/20/10	0	1
PP/EPR/BaSO <sub>4</sub>	70/20/10	1	1
PP/EPR/BaSO <sub>4</sub>	70/20/10	2.5	1
PP/EPR/BaSO <sub>4</sub>	70/20/10	5	1
PP/EPMA/BaSO <sub>4</sub>	70/20/10	0	1
PP/EPMA/BaSO <sub>4</sub>	70/20/10	0	0.7
PP/EPMA/BaSO <sub>4</sub>	70/20/10	0	0.1
PP	100	0	—
PP/MAPP	97.5/2.5	2.5	—
PP/MAPP	95/5	5	—
PP/BaSO <sub>4</sub>	90/10	0	1
PP/BaSO <sub>4</sub>	90/10	0	0.7
PP/BaSO <sub>4</sub>	90/10	0	0.1
PP/EPR	80/20	0	—
PP/EPR	70/30	0	—
PP/EPMA	80/20	0	—
PP/EPMA	70/30	0	—

<sup>a</sup>Volume percentage of the PP matrix.

analysis were carried out on tensile bars (150 × 10 × 4 mm) injection molded on a Battenfeld BA 200/50 CD machine.

The structure of the samples was characterized by dynamic mechanical analysis. The measurements were carried out on a Rheometrics Dynamic Analyzer RDAII with a rectangular torsion fixture at 1 rad/s. Scanning electron microscopic analysis was performed with a Zeiss DSM 940A apparatus on samples fractured at liquid nitrogen temperature. Fracture surfaces were etched by immersing them in n-heptane for 1 min. Tensile testing was carried out on Zwick 1445 equipment with a 50 mm/min cross head speed and 115 mm gauge length. Young's modulus was determined at a 1% deformation. Flexural strength and modulus were measured on the same apparatus. Notched Charpy impact strength (notch radius 0.25 mm) was determined at a rate of 2.9 m/s on 80 × 10 × 4 mm specimens cut from the injection molded tensile bars.

## 4. Results and discussion

The properties of the three-component system investigated are determined mainly by their structure. Besides the spatial distribution of the components, another structure-related factor must be considered, the aggregation of small filler particles. The properties are also influenced by factors as, for example, the strength of interfacial interaction, which has a considerable effect on properties measured at large deformations (tensile, impact). These questions will be discussed in two main sections dealing with structure and properties, respectively.

### 4.1. Structure

Encapsulation or separate dispersion is the most important question of the structure in these three-components systems, as was discussed above. Dynamic mechanical spectroscopy, or generally the measurement of dynamic modulus and phase angle,  $\delta$ , is the best technique for the

characterization of the morphology [12, 21–24]. Fillers increase modulus, while the addition of elastomers decreases it. Encapsulated filler particles behave similarly to the elastomer itself, since the filler extends the amount of elastomer present. This can be very sensitively detected by the intensity of the glass transition of the elastomer phase appearing at around  $-50^\circ\text{C}$  on the dynamic mechanical spectra. In the neat polypropylene or the composite containing only the filler, no transition is detected in the temperature range between  $-70$  and  $-20^\circ\text{C}$ . In the blend containing 20 vol % elastomer, the transition of the elastomer is very pronounced, and the intensity of the transition (height of  $\tan \delta$  peak) is proportional to the relaxing material (Fig. 1). The intensity of this transition is slightly lower in the three-component system containing the 1  $\mu\text{m}$  filler particles and EPR elastomer, in spite of the fact that the same amount of elastomer is present. The addition of 1% functionalized PP lead to the incorporation of the fillers in the polypropylene phase and the loss maximum is identical with the maximum of a 20 vol % elastomer filled polypropylene. Extensive encapsulation of the filler by the functionalized elastomer, maleic anhydride grafted ethylene-propylene rubber leads, however, to a large increase in the amount of relaxing material. The filler extends the elastomer, apparently increasing its amount, see Fig. 1. A quantitative theoretical evaluation of the maximum of  $\tan \delta$ , using the interlayer model [12, 20], is not possible in this case, because the model is only applicable to isotropic materials. Anisotropy is a result of the injection molding process, and differences in melt viscosity can be expected.

The relative modulus change of the composites is presented in Fig. 2 for the injection molded samples of various composition. The expected tendency is shown by the individual components; the elastomer decreases, while the filler increases the stiffness of PP. The modulus of the three-component system (3PP) is much smaller than that of the filled composite. In the case of additivity, a somewhat larger modulus could be expected. It cannot be excluded that limited encapsulation of the filler also takes place in the absence of functionalized components. The introduction of functionalized PP (3MAPP) should lead to separate dispersion of the

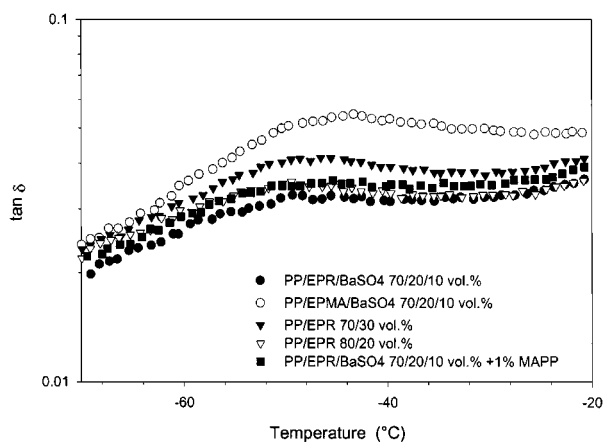


Figure 1 Dependence of the  $\tan \delta$  of PP composites on temperature in the relaxation transition range of the EP phase; particle size: 1  $\mu\text{m}$ . Frequency: 1 rad/s.

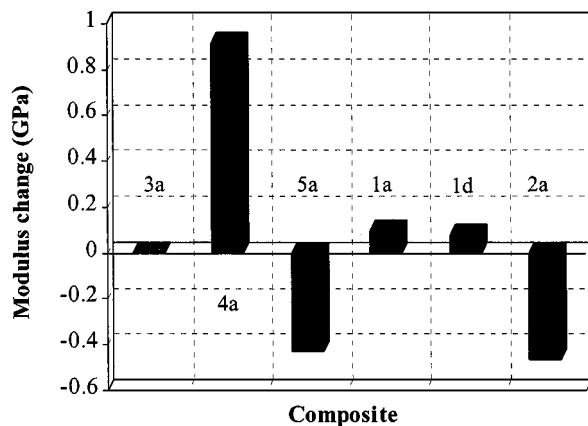


Figure 2 Dependence of Young's modulus on composition, relative change compared to PP: (EPR) PP/EPR 80/20 vol%, (BaSO<sub>4</sub>) PP/BaSO<sub>4</sub> 90/10 vol%, (3PP) PP/EPR/BaSO<sub>4</sub> 70/20/10 vol%, (3MAPP) PP/EPR/BaSO<sub>4</sub> 70/20/10 vol% plus MAPP and (3MAEP) PP/EPMA/BaSO<sub>4</sub> 70/20/10 vol%. Particle size: 1  $\mu$ m.

components. The incorporation of EPMA results in encapsulation, and the modulus decreases below the value of the PP/EPR blend, in accordance with the results of the dynamic mechanical analysis.

SEM analysis further supports the results of DMA and mechanical measurements. The fracture surface of the PP/EPR/BaSO<sub>4</sub> composite is shown in Fig. 3a. The composite contained 1.0  $\mu$ m particles, and the surface was etched with n-heptane. The separately dispersed filler particles are clearly visible on the surface, while matrix/filler adhesion is weak. The number of voids

is about the same in the SEM micrograph, in Fig. 3b, taken from the fracture surface of the composite containing 1% maleic anhydride grafted polypropylene, but the adhesion between the filler and the matrix is much stronger, which is why filler particles are absent from the surface. Fig. 3c shows the fracture surface of the corresponding composite containing EPMA. The number of independent voids representing the etched-off elastomer is low, and separate filler particles cannot be detected on the surface, as they are encapsulated in the elastomer.

The results of all experiments are in complete agreement and clearly show that encapsulation of the filler particles takes place with the introduction of the functionalized elastomer into the composite. Secondly, the incorporation of MAPP in the filled blend results in increased adhesion between the PP matrix and the filler [12].

The other structure-related phenomenon that must be considered here is the aggregation of small filler particles. Aggregation was not detected in composites containing the filler with the two larger average particle sizes (1.0 and 0.7  $\mu$ m), but considerable aggregation was observed in the case of the small filler particles (0.1  $\mu$ m). This is clearly demonstrated by Fig. 4, showing the fracture surface of the composite containing the small particles. The absence of voids indicates strong encapsulation again, but it is also clear that the composite contains large aggregates. The presence of aggregates deteriorates properties, as will be shown in the next section.

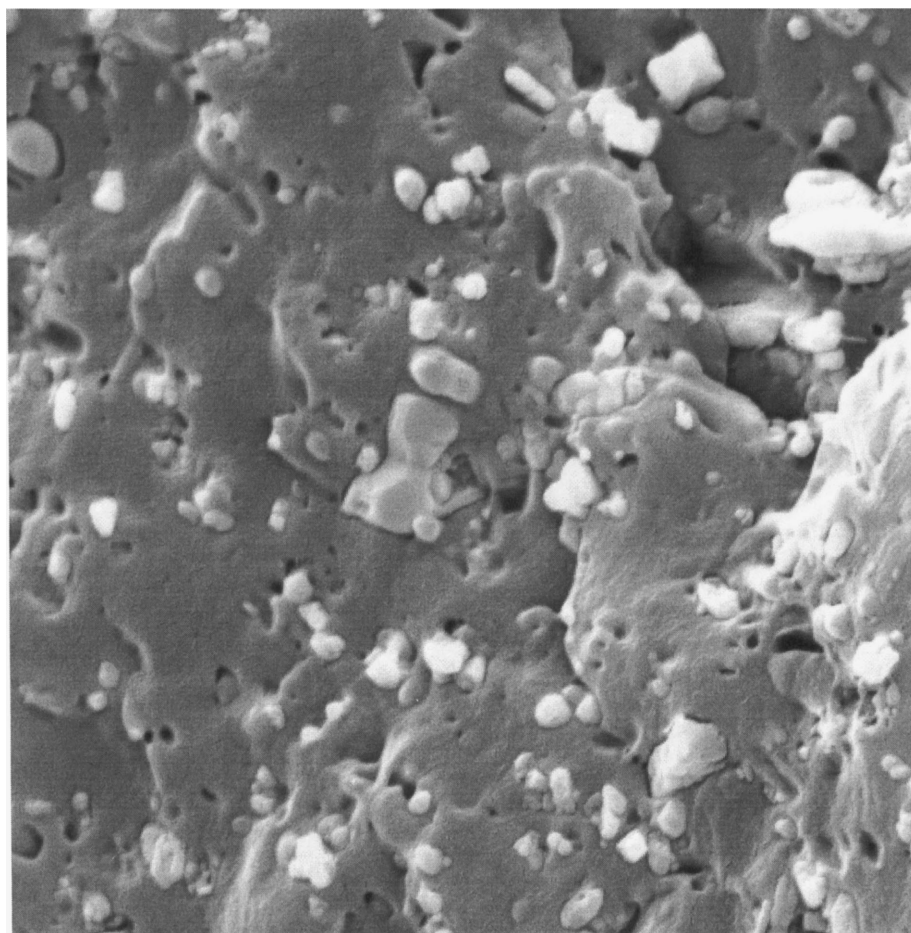
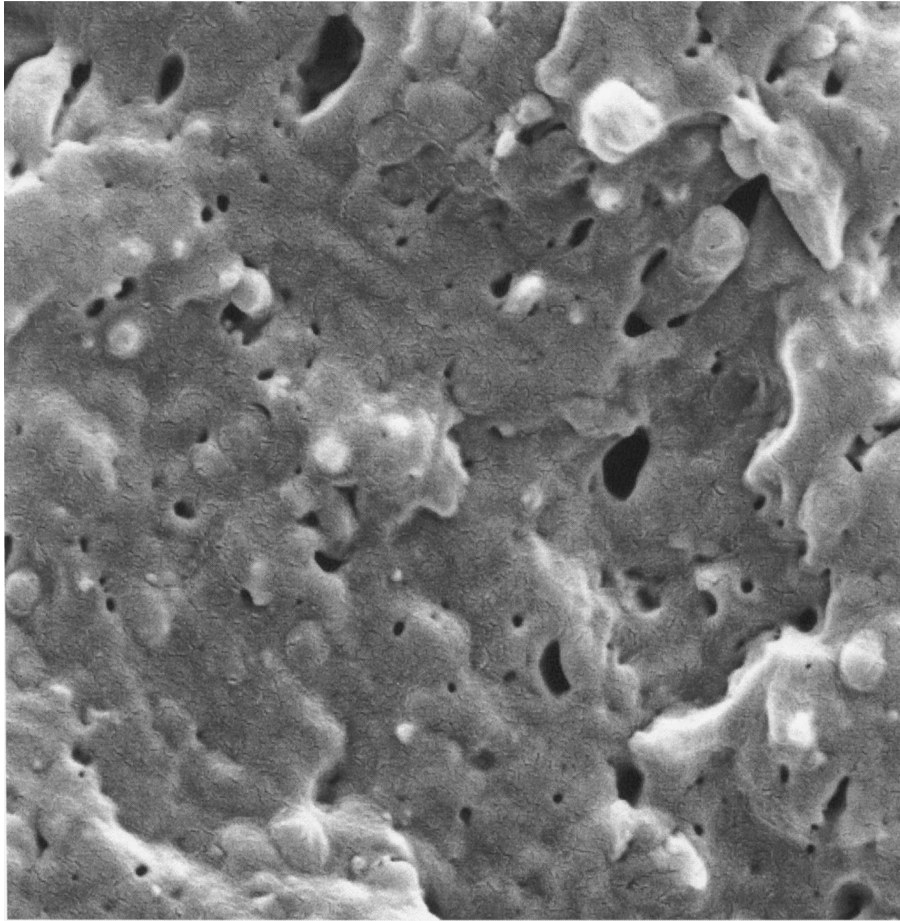
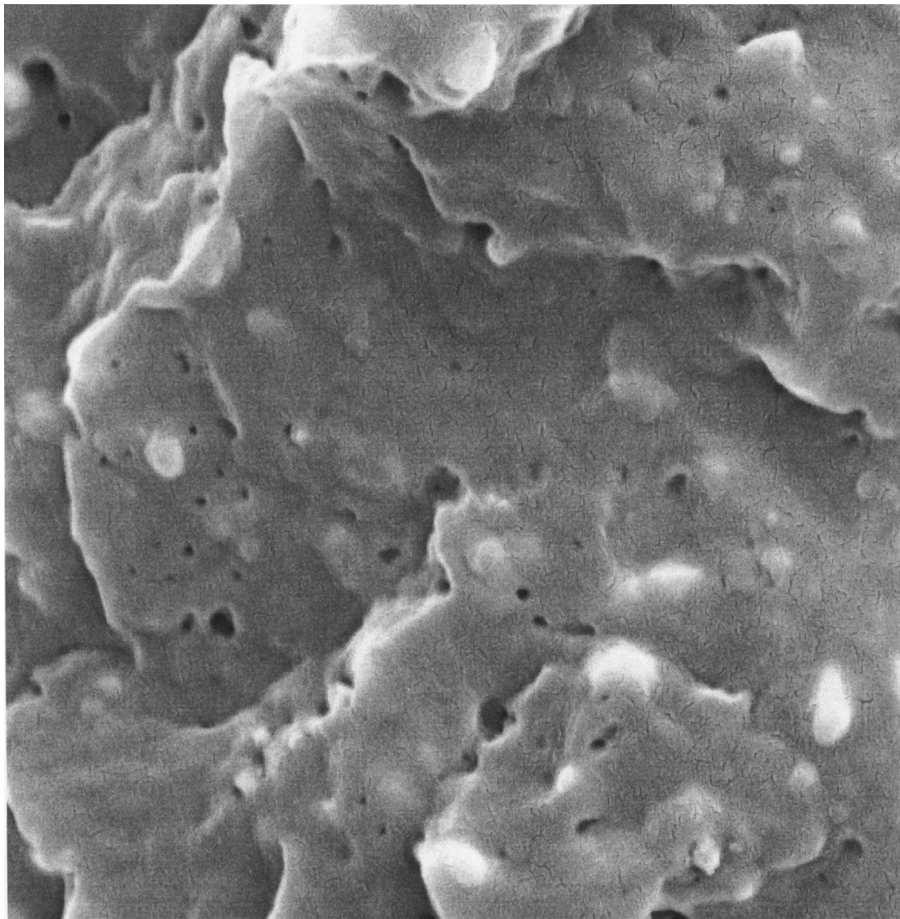


Figure 3a SEM micrograph taken from the etched fracture surface of a PP/EPR/BaSO<sub>4</sub>-70/20/10 composite; particle size: 1.0  $\mu$ m.



*Figure 3b* SEM micrograph taken from the etched fracture surface of a PP/EPR/BaSO<sub>4</sub>-70/20/10 composite containing 1.0 vol % MAPP; particle size: 1.0  $\mu$ m.



*Figure 3c* SEM micrograph taken from the etched fracture surface of a PP/EPMA/BaSO<sub>4</sub>-70/20/10 composite; particle size: 1.0  $\mu$ m.

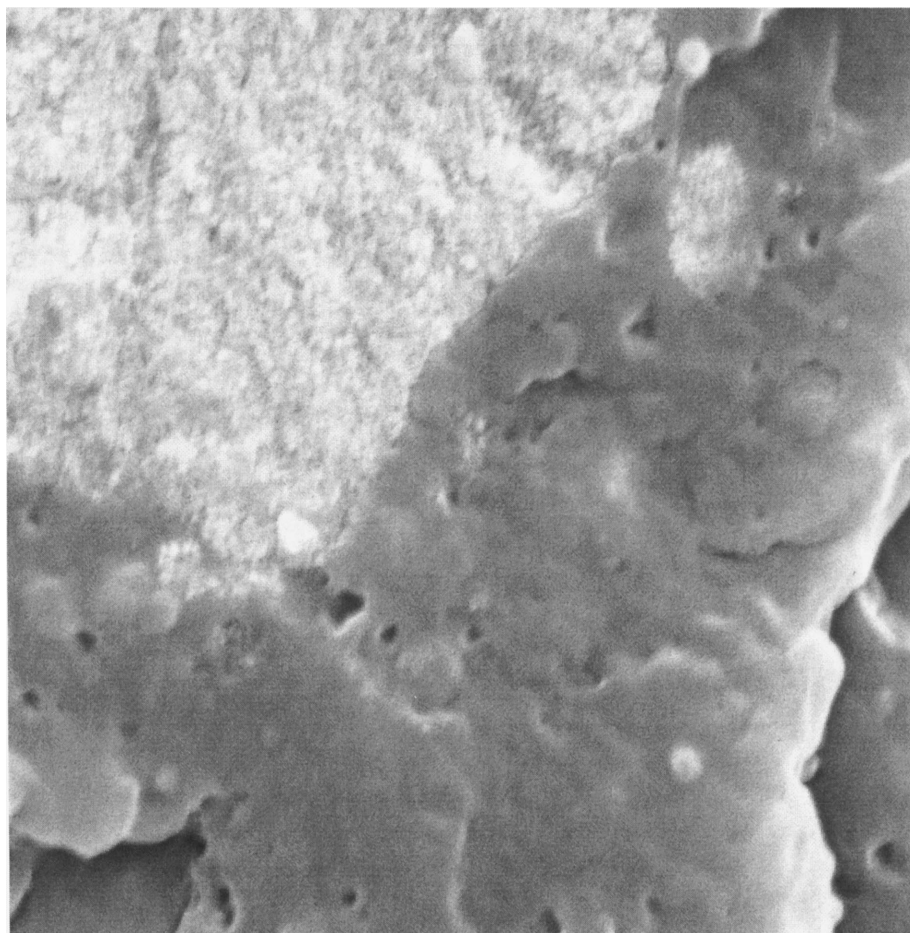


Figure 4 Encapsulation and aggregation of small particles in a PP/EPMA/BaSO<sub>4</sub>-70/20/10 composite; particle size: 0.1 μm. The aggregate is the light region in the top left of the field of view.

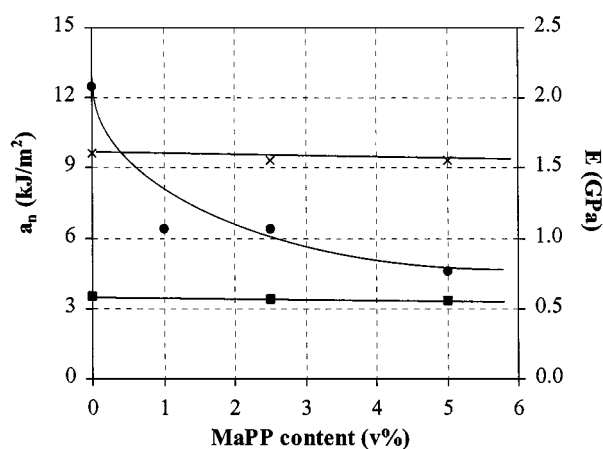


Figure 5 Dependence of stiffness and toughness of PP and the composites on their MAPP content; (□) impact strength,  $a_n$ -PP, (×) Young's modulus,  $E$ -PP/EPR/BaSO<sub>4</sub>-70/20/10, (○)  $a_n$ -PP/EPR/BaSO<sub>4</sub>-70/20/10; particle size: 1.0 μm.

## 4.2. Properties

The structure of the composites determines their properties, but, as mentioned earlier, other factors also influence them. This statement is strongly supported by Fig. 5, where the Young's modulus and notched Charpy impact resistance of some of the three-component system (PP/EPR/BaSO<sub>4</sub>) is plotted as a function of MAPP content. Modulus does not change, which clearly proves that the filler is mainly present in the PP matrix

phase with and without the maleinated PP. The MAPP content of the composite does not influence the impact resistance of the matrix polymer either. However, the impact strength of the composites in Fig. 5 decreases substantially with an increasing amount of MAPP in the blend. The decrease is a result of improving matrix/filler adhesion, which leads to decreased deformability of the polymer. In composites containing particulate fillers, impact resistance usually increases due to the energy absorption of the new micromechanical deformation process, debonding. Impact resistance decreases with increasing adhesion, as shown previously [25].

A further proof of increased adhesion is supplied by the dependence of tensile yield stress on the amount of MAPP in the composite (Fig. 6). The correlation is very similar to that shown by the impact resistance, but opposite in direction, i.e. yield stress increases as the amount of MAPP increases.

In particulate filled polymers containing filler particles in the usual size range, i.e. around 1–3 μm average particle size, the dominating micromechanical deformation process is debonding. This leads to a decrease in tensile yield stress with increasing filler content. The rate of decrease depends on the relative load-bearing capacity of the filler, on its specific surface area, and on adhesion [26]. The tensile yield stress of some of the composites was plotted as a function of the volume fraction of the two additional components in Fig. 7. The theoretical minimum can be calculated

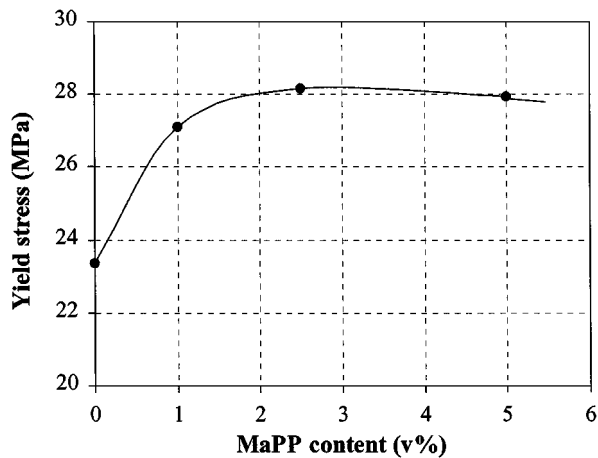


Figure 6 Effect of MAPP content on the tensile yield stress of PP/EPR/BaSO<sub>4</sub>-70/20/10 composites; particle size: 1.0 μm.

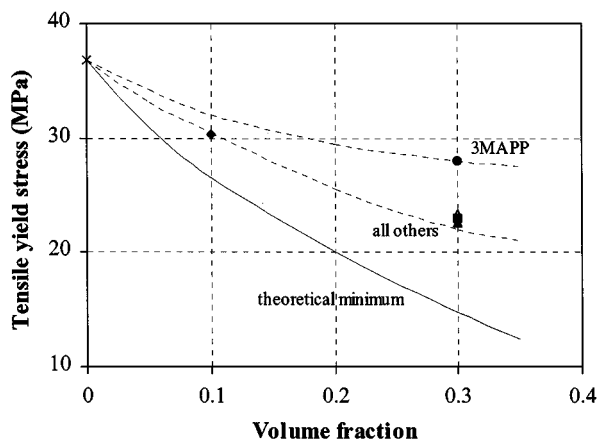


Figure 7 Composition dependence of tensile yield stress of PP blends and composites, effect of adhesion; (×) PP, (◇) PP/BaSO<sub>4</sub>, (○) 3MAPP-PP/EPR composite containing MAPP, (△) PP/EPR, (□) 3EPMA-PP/EPMA composite, (+) 3PP-PP/EPR/BaSO<sub>4</sub> composite.

from an existing model by assuming zero interaction of the components [27, 28]. Although the number of points is limited, it is clear that the composite containing MAPP has increased adhesion. All the other blends and composites demonstrate the same correlation, indicating that the load-bearing capacity of the dispersed components is identical. The probability of filler aggregation greatly increases with decreasing particle size. Aggregation usually leads to the deterioration of properties. Aggregates act as fracture initiation sites under dynamic conditions, and impact resistance and all properties measured at large deformations decrease [29]. This is demonstrated well by Figs 8 and 9, showing the particle size dependence of the elongation-at-break and notched Charpy impact strength of the composites. Both correlations are very similar to each other, showing a maximum at 0.7 μm particle size. Small filler particles strongly aggregate, leading to a substantial decrease in both properties. The aggregates are typically larger than 1 μm and fall apart during fracture, while the larger filler particles debond. This explains the particle size dependence observed in Figs 8 and 9.

Finally, an important aspect of all such studies is the optimization of properties. The increase in modulus is usually accompanied by a decrease in impact

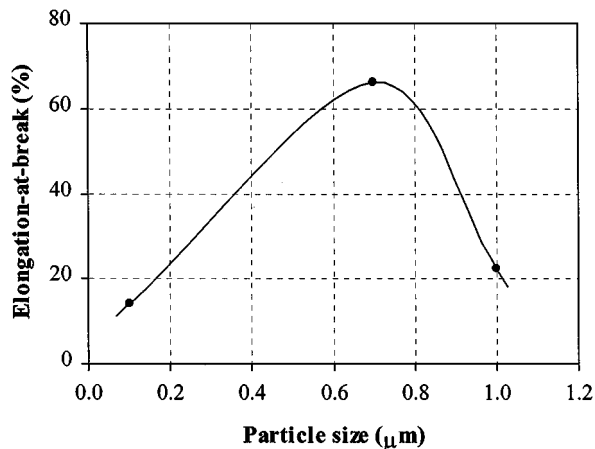


Figure 8 Effect of filler particle size on the elongation-at-break of PP/EPMA/BaSO<sub>4</sub>-70/20/10 composites; particle size: 0.1, 0.7 and 1.0 μm.

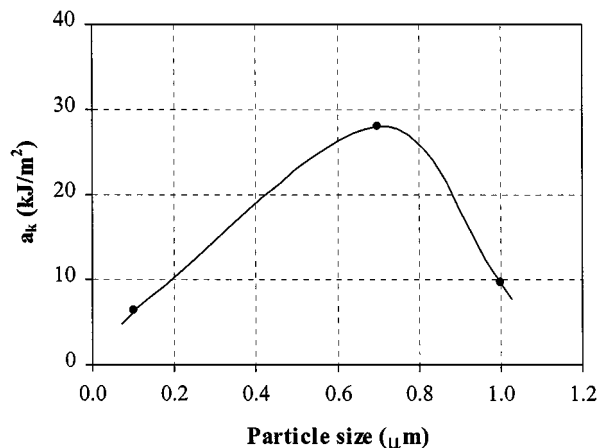


Figure 9 Effect of aggregation on the impact strength of PP/EPMA/BaSO<sub>4</sub>-70/20/10 composites; particle size: 0.1, 0.7 and 1.0 μm.

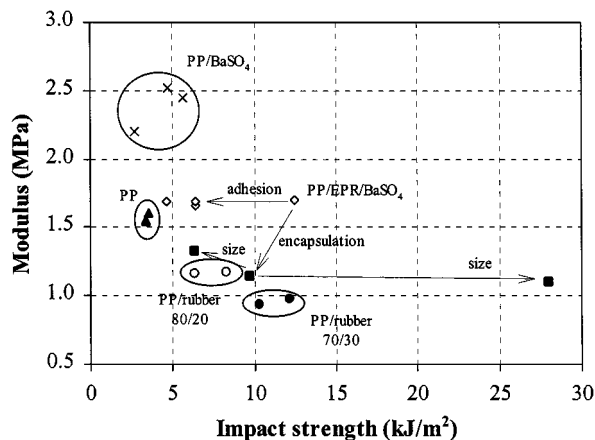


Figure 10 Effect of various factors on the stiffness and toughness of three-component PP composites; property optimization.

resistance, but an increase in both characteristics is demanded in practice. The effect of the studied factors on the two properties is presented in Fig. 10. Filler does indeed increase stiffness and decrease impact strength, and the elastomer has the opposite effect. Increased adhesion leads to decreased impact resistance, while encapsulation results in an increase in this property, but modulus substantially decreases as a consequence. A decrease in the BaSO<sub>4</sub>-filler particle size from

1 to 0.7  $\mu\text{m}$  in the PP/EPMA/BaSO<sub>4</sub> system enhances the impact resistance at approximately constant modulus, as can be seen in Fig. 10. The proper selection of filler particle size and the introduction of functionalized polymers may lead to the desired combination of properties, i.e. to tailor-made composites.

## 5. Conclusions

The structure and properties of various three-component PP/EPR/BaSO<sub>4</sub> systems can be controlled when standard processing methods, as extrusion and injection molding, are applied. The aspect of structure control concerned was the separate dispersion of filler and rubber in the PP matrix or encapsulation of the filler in the rubber phase. The former structure prevails in the PP/EPR/BaSO<sub>4</sub> systems, and addition of MAPP enhances the adhesion between the PP matrix and the filler. Encapsulation of the filler particles into the elastomer takes place when maleated rubber is used, and the encapsulated structure prevails even under the severe shearing conditions of injection molding. The improved matrix/filler adhesion resulted in increased yield stress and tensile strength, but decreased impact resistance. The particle size of the filler proved to be a crucial factor; below a certain particle size aggregation becomes a dominating factor. Extensive aggregation leads to the deterioration of all mechanical properties, especially to decreased impact strength. Proper selection of components and composition may lead to an optimum in the combination of properties.

## Acknowledgement

The authors gratefully acknowledge the National Swedish Board for Industrial and Technical Development (NUTEK) for financial support of this work. The National Scientific Research Fund of Hungary (Grant No. T 016500) is also acknowledged for its financial contribution. We are also grateful to V. Blomquist for her assistance with the preparation of the composites and execution of DMA measurements, to A. Mårtenson for SEM studies, to L. I. Kulin and M. Björklund for the GPC and to M. Ågren for the DSC measurements.

## References

1. J. KARGER-KOCSIS, "Polypropylene. Structure, Blends and Composites" (Chapman and Hall, London, 1985).

2. Mitsubishi Kagaku KK, JP 07118462-Impact-resistant and rigid automobile bumpers made of polyolefin compositions-Mitsubishi Kagaku Kk, Japan; Nissan Motor.
3. Sumitomo Chemical Co. Ltd., EP 580069-Injection molding compositions for automobile bumpers-Sumitomo Chemical Co. Ltd., Japan; Toyota Jidosha Kabushiki Kaisha.
4. Idemitsu Petrochemical Co. Ltd., JP 02251547-Polyolefin compositions for automobile bumpers-Idemitsu Petrochemical Co. Ltd., Japan.
5. J. JANCÁR and A. T. DIBENEDETTO, *J. Mater. Sci.* **30** (1995) 2438.
6. *Idem.*, *ibid.* **30** (1995) 1601.
7. E. K. L. LAU, *SPE ANTEC* **50**(1) (1992) 310.
8. G. MAROSI, G. BERTALAN, P. ANNA and I. RUSZNÁK, *J. Polym. Eng.* **12** (1993) 33.
9. W.-Y. CHIANG, W.-D. YANG and B. PUKÁNSZKY, *Polym. Eng. Sci.* **34** (1994) 485.
10. E. LAU and J. GOODMAN, *J. Elastomers Plast.* **25** (1993) 322.
11. B. PUKÁNSZKY, F. TÜDŐS, J. KOLÁRÍK and F. LEDNICKÝ, *Polym. Compos.* **11** (2) (1990) 98.
12. C. O. HAMMER and F. H. J. MAURER, *J. Adhesion* **64** (1997) 61.
13. C. O. HAMMER and F. H. J. MAURER, *Polym. Compos.* **19** (1998) 116.
14. *Idem.*, *Comp. Interfaces* **5** (1998) 241.
15. J. KOLÁRÍK, F. LEDNICKÝ and B. PUKÁNSZKY, Proceedings of 6th ICCM/2nd ECCM, edited by F. L. Matthews, N. C. R. Buskell, J. M. Hodgkinson and J. Morton (Elsevier, London, 1987) vol. 1., p. 452.
16. D. TABOR, in "Tribology in Particulate Technology," edited by B. J. Briscoe and M. J. Adams (Adam Hilger, Bristol, 1987) p. 206.
17. M. J. ADAMS and B. EDMONDSON, in "Tribology in Particulate Technology," edited by B. J. Briscoe and M. J. Adams (Adam Hilger, Bristol, 1987) p. 154.
18. S. L. GOREN, *J. Colloid Interface Sci.* **36** (1971) 94.
19. B. PUKÁNSZKY, F. TÜDŐS, J. KOLÁRÍK and F. LEDNICKÝ, *Compos. Polym.* **2** (1989) 491.
20. F. H. J. MAURER, in "Polymer Composites," edited by B. Sedláček (Walter de Gruyter, Berlin, 1986) p. 399.
21. A. L. PERSSON and H. BERTILSSON, *Polymer* **18** (1998) 4183.
22. *Idem.*, *ibid.* **23** (1998) 5633.
23. D. QUINTENS, G. GROENINCKX, M. GUEST and L. AERTS, *Polym. Eng. Sci.* **30** (1990) 1474.
24. *Idem.*, *ibid.* **31** (1991) 1207.
25. B. PUKÁNSZKY and F. H. J. MAURER, *Polymer* **36** (1995) 1617.
26. B. PUKÁNSZKY, in Ref. 1, 3, p. 1-70.
27. B. PUKÁNSZKY, B. TURCSÁNYI and F. TÜDŐS, in "Polymer, Ceramic, and Metal Matrix Composites," edited by H. Ishida (Elsevier, New York, 1988) p. 467.
28. B. PUKÁNSZKY, *Composites* **21** (1990) 255.
29. V. SVEHLOVA and E. POLOUCEK, *Angew. Makromol. Chem.* **153** (1987) 197.

Received 24 November 1997

and accepted 13 January 1999